Combined Particle/FIR Filtering for Indoor Localization Based on Wireless Sensor Networks

JUNG MIN PAK, CHOON KI AHN, MYO TAEG LIM
Korea University
School of Electrical Engineering
145, Anam-ro, Seongbuk-gu, Seoul
REPUBLIC OF KOREA

YURIY S. SHMALIY
Universidad de Guanajuato
Department of Electronics Engineering
Salamanca, 36885
MEXICO

Abstract: In this paper, we propose a new nonlinear f ltering algorithm that can provide more accurate and reliable localization compared with the pure particle f ltering (PF). In the proposed algorithm, failures of the PF are detected, and the failed PF is recovered using a f nite impulse response (FIR) f lter. The resulting f lter is called the combined particle/FIR f lter (CPFF). We demonstrate the performance of the CPFF by the indoor human localization.

Key–Words: Localization, particle f lter, f nite impulse response (FIR) f lter, combined particle/FIR f lter.

1 Introduction

Indoor localization systems have attracted attention of engineers and users in recent years. Indoor localization technologies based on wireless sensor networks (WSNs) have been used for various purposes, such as tracking workers in construction sites, human localization in intelligent buildings, and cargo tracking in logistics [1–3]. Indoor localization systems usually take advantage of f ltering technologies in order to suppress the bad effect of measurement noise [4–6]. The f lters, such as the extended Kalman f lter (EKF) and the particle f lter (PF), assist the localization systems to produce accurate position information in noisy environment.

In particular, the PF has been popularly used for localization systems. This is because the PF has many advantages, for example, it can work without information on the initial position, which is diff cult for the EKF [6]. However, the PF has the serious drawback that it often exhibits localization failures due to sample impoverishment [6, 7]. Diverse versions of the PFs, such as the regularized PF (RPF) [8], Markov chain Monte Carlo (MCMC) move step [9], and unscented PF [10], were developed to overcome the PF failure and sample impoverishment [11]. Although the existing versions of the PFs can alleviate sample impoverishment, they cannot recover the algorithm from failures.

In this paper, we propose a new nonlinear f ltering algorithm, which can provide more accurate and reliable localization compared with the pure PF. In the proposed algorithm, we use the f nite impulse response (FIR) f lter [12–30]. The key feature of the FIR f lter is that it uses only recent f nite measurements. In contrast, inf nite impulse response (IIR) f lters, such as the EKF and the PF, use all past measurements. In the IIR f lter structure, modeling and computational errors accumulate over time, which causes failure or f lter divergence. Since the FIR f lter uses only f nite measurements, it can prevent accumulation of modeling and computational errors. Moreover, the FIR f lter has built-in bounded-input bounded output (BIBO) stability.

In the proposed algorithm, we use the PF as a main f lter, because the IIR-type f lters are more accurate than FIR f lters under ideal conditions. When modeling and computational errors are negligible, the PF provides more accurate localization than the FIR f lter. However, when the PF algorithm fails due to sample impoverishment, we use a nonlinear FIR f lter as an assisting f lter. When PF failures are detected, the failed PF is reset using the output of the assisting nonlinear FIR f lter. In this way, the PF algorithm can be recovered from failures. The proposed f ltering algorithm is called the combined particle/FIR f ltering (CPFF) [31]. We apply the CPFF to the indoor localization based on WSN and demonstrate the performance of the CPFF in a comparison with the pure PF.

The remainder of this paper is organized as follows. In Section 2, indoor localization based on WSN is explained. In Section 3, the CPFF algorithm is presented. In Section 4, we test the CPFF by the indoor localization and conclusion is drawn in Section 5.

2 Indoor Localization Based on WSN

In this section, a typical scheme of indoor localization based on WSN is explained. The localization using the PF requires the motion and measurement models. We assume that the target object is a person. In this case, the random-walk motion model [32] is typically used. We assume that the 2D positions and velocities of the person are represented by (x, y) and $(\dot{x}, \dot{y})$, respectively. The motion of the person is then represented by the following equations:

$$x_k = x_{k-1} + T\dot{x}_{k-1}, \tag{1}$$

$$y_k = y_{k-1} + T\dot{y}_{k-1}, \tag{2}$$

$$\dot{x}_k = \dot{x}_{k-1}, \tag{3}$$

$$\dot{y}_k = \dot{y}_{k-1}, \tag{4}$$

where T is the sampling time.

Figure 1 sketches the 2D schematic of indoor person localization. A mobile tag (transmitter) is attached to the person. Four receivers are installed at fixed positions. We use the time-of-arrival (TOA) measurement, which is the time interval required by a signal to pass from the tag to the receiver. Note that the receiver's exact coordinates (x_i, y_i), $i = 1, 2, 3, 4$, are supposedly known. The TOA measurement model is described as follows:

$$z_{i,k} = \frac{1}{c}\sqrt{(x_k - x_i)^2 + (y_k - y_i)^2}, \tag{5}$$

where $z_{i,k}$ denotes the TOA measurements and c refers to the speed of light.

By introducing a state vector $\mathbf{x}_k = [x_k \ y_k \ \dot{x}_k \ \dot{y}_k]^T$, the motion of the person can be modeled in a state-space form as follows:

$$\begin{aligned}\mathbf{x}_k &= \mathbf{f}_{k-1}(\mathbf{x}_{k-1}, \mathbf{w}_{k-1}) \\ &= \begin{bmatrix} 1 & 0 & T & 0 \\ 0 & 1 & 0 & T \\ 0 & 0 & 1 & 0 \\ 0 & 0 & 0 & 1 \end{bmatrix} \mathbf{x}_{k-1} \\ &+ \begin{bmatrix} T^2/2 & 0 \\ 0 & T^2/2 \\ T & 0 \\ 0 & T \end{bmatrix} \mathbf{w}_{k-1}, \end{aligned} \tag{6}$$

where $\mathbf{w}_{k-1} \in \Re^2$ is the process noise vector with the covariance $\mathbf{Q}_{k-1}$. Note that the motion model (i.e., random-walk model) is linear. In turn, assigning a measurement vector $\mathbf{z}_k = [z_{1,k} \ z_{2,k} \ z_{3,k} \ z_{4,k}]^T$ allows modeling the TOA measurement in state space as

$$\mathbf{z}_k = \mathbf{h}_k(\mathbf{x}_k) + \mathbf{v}_k, \tag{7}$$

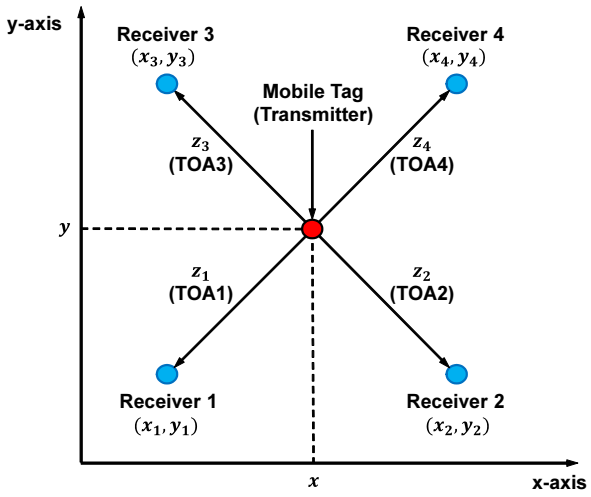

Figure 1: 2D schematic indoor floor space geometry of a mobile tag and four receivers.

where $\mathbf{h}_k = [h_{1,k} \ h_{2,k} \ h_{3,k} \ h_{4,k}]^T$ has the components

$$h_{i,k} = \frac{1}{c}\sqrt{(x_k - x_i)^2 + (y_k - y_i)^2}, \ \ (i = 1, 2, 3, 4), \tag{8}$$

and $\mathbf{v}_k \in \Re^4$ is a zero-mean measurement noise vector having the covariance $\mathbf{R}_k$.

Provided (6) and (7), the 2D location and velocity of the person can be estimated using the PF. Diverse PF algorithms are available, in this paper, we use the RPF [8]

3 Combined Particle/FIR Filtering

The key idea of the CPFF is to reset a failed PF using a nonlinear FIR filter when PF failure is detected. At each time index k, the PF operates in a standard mode, and its output is tested for failures. When an abnormal operation of the PF is detected, the nonlinear FIR filter is operated. Using the output of the FIR filter, the PF is reset and rebooted. The detailed algorithms of the CPFF is presented in [31]. In this paper, we explain only key processes of the CPFF.

3.1 Detection of PF Failure

The detection of PF failure is the most important process in the CPFF. In this subsection, we propose a simple and effective algorithm for the detection of PF failure.

The PF produces the estimated state, which is denoted by $\hat{\mathbf{x}}_k$. Using the measurement model and the estimated state, we can obtain the estimated measurement denoted by $\hat{\mathbf{z}}_k$. In (7), assuming $\mathbf{v}_k = \mathbf{0}$ and sub-

stituting $\hat{\mathbf{x}}_k$ for $\mathbf{x}_k$, we obtain $\hat{\mathbf{z}}_k$. The real measurement system, WSN, generates the actual TOA measurement, $\mathbf{z}_k$. The residual, $\mathbf{r}_k$, is def ned as the difference between the estimated measurement and the actual measurement. By evaluating the residual, we can diagnose the abnormality of the PF's output. Since the WSN generally provides very accurate measurements, we trust the real measurements. If the estimated measurement is far from the actual measurement, we assume that the PF's output is inaccurate. To evaluate the difference between $\hat{\mathbf{z}}_k$ and $\mathbf{z}_k$, we use the *Mahalanobis* distance [33], which is def ned as

$$\begin{aligned}\mathcal{D}_k &\triangleq (\mathbf{z}_k - \hat{\mathbf{z}}_k)^T \mathbf{R}_k^{-1} (\mathbf{z}_k - \hat{\mathbf{z}}_k), \\ &= \mathbf{r}_k^T \mathbf{R}_k^{-1} \mathbf{r}_k, \end{aligned} \tag{9}$$

where $\mathbf{R}_k$ is the measurement noise covariance.

A measurement system with Gaussian measurement noise has an error bound (or uncertainty bound) that is represented by an ellipsoid in the case of 2D space [34]. Given the conf dence level for the measurement system, the *Mahalanobis* distance between $\mathbf{z}_k$ and a point on the error bound can be found in the *chi-square* table [35], and it is used as a threshold value when evaluating $\mathcal{D}_k$. For example, if the conf - dence level is 99% and the dimension of the measurement vector is 4, the *chi-square* value is 13.28, which is used as the threshold denoted by T_D. If $\mathcal{D}_k$ is larger than T_D, it means that the estimated measurement is beyond the error bound. In this case, we judge that the PF is in failure. The output of the decision-making system is the indicator variable, I_k. When PF failure is detected, the output is represented as $I_k = 1$. When PF failure is not detected the output is $I_k = 0$. The choice of the threshold determines the failure decision sensitivity and false alarm rate. Thus, T_D must be set to a suff ciently large value in order to avoid false alarms. We recommend using the *chi-square* values corresponding to the 99% conf dence.

3.2 Algorithm of the CPFF

The CPFF is the combination of the PF and the nonlinear FIR f lter. When PF failure is detected, the PF is reset by using the output of the nonlinear FIR f lter. The estimated state, $\hat{\mathbf{x}}_{k,\mathrm{FIR}}$, and the estimation error covariance, $\mathbf{P}_{k,\mathrm{FIR}}$, which are obtained from the FIR f lter, can be used as the mean and covariance of the Gaussian distribution, respectively. Then, following the obtained Gaussian distribution, new random samples of states (i.e., particles) can be generated as follows:

$$\hat{\mathbf{x}}_k^i \sim \mathcal{N}(\hat{\mathbf{x}}_{k,\mathrm{FIR}}, \mathbf{P}_{k,\mathrm{FIR}}). \tag{10}$$

Algorithm 1: CPFF

begin
- Generate N initial particles for particle f ltering.
- **for** $k = 1, 2, \cdots$ **do**
  - Perform particle f ltering using the RPF [8], and obtain the estimated state $\hat{\mathbf{x}}_{k,\mathrm{PF}}$.
  - $\hat{\mathbf{x}}_k = \hat{\mathbf{x}}_{k,\mathrm{PF}}$
  - **if** $k \geq M + 1$ **then**
    - Compute the estimated measurement: $\hat{\mathbf{z}}_k = \mathbf{h}_k(\hat{\mathbf{x}}_{k,\mathrm{PF}})$
    - Compute the Mahalanobis distance $\mathcal{D}_k$ between the estimated measurement $\hat{\mathbf{z}}_k$ and the actual measurement $\mathbf{z}_k$: $\mathcal{D}_k = (\mathbf{z}_k - \hat{\mathbf{z}}_k)\mathbf{R}_k^{-1}(\mathbf{z}_k - \hat{\mathbf{z}}_k)$.
    - **if** $\mathcal{D}_k > T_D$ **then**
      - Perform nonlinear FIR f ltering using the EMVFF [23], and obtain $\hat{\mathbf{x}}_{k,\mathrm{FIR}}$ and $\mathbf{P}_{k,\mathrm{FIR}}$.
      - $\hat{\mathbf{x}}_k = \hat{\mathbf{x}}_{k,\mathrm{FIR}}$
      - Generate new particles using Gaussian distribution and reset the PF: $\hat{\mathbf{x}}_k^i \sim \mathcal{N}(\hat{\mathbf{x}}_{k,\mathrm{FIR}}, \mathbf{P}_{k,\mathrm{FIR}})$
    - **end if**
  - **end if**
- **end for**

end

† N denotes the number of particles used in particle f ltering.

† M denotes the horizon size, which is an important design parameter of the FIR f lter.

† $\hat{\mathbf{x}}_{k,\mathrm{PF}}$ denotes the state estimate obtained from the particle f ltering, and $\hat{\mathbf{x}}_k^i$ $(i = 1, 2, \cdots, N)$ denotes the particles used in the particle f ltering.

† $\hat{\mathbf{x}}_k$ is the output (state estimate) of the CPFF.

The newly generated particles are used for the PF instead of the old particles. In this way, the resetting of the PF is implemented. In this paper, we construct the CPFF using the RPF [8] and the extended minimum variance FIR f lter (EMVFF) [23]. The algorithm of the RPF and the EMVFF can be found in [8] and [23], respectively. The algorithm of the CPFF can be summarized by *Algorithm* 1.

4 Indoor Localization Based on WSN via CPFF

In this section, we apply the CPFF to indoor localization based on WSN. We compare the localization errors produced by the CPFF (*Algorithm* 1) and the pure PF (i.e, RPF). A simulation scenario is sketched in Fig. 2(a). Here, four receivers are installed at exact positions $(0,0),(10,0),(0,10),(10,10)$, all in meters. A person departs from the position $(3,3)$ and moves counterclockwise along a rectangular trajectory. The design parameters are set as follows. The process and measurement noise covariance matrices are taken as

$$\mathbf{Q}_k = \sigma_w^2 \mathbf{I}_2, \quad \sigma_w = 0.1, \tag{11}$$

$$\mathbf{R}_k = \sigma_v^2 \mathbf{I}_4, \quad \sigma_v = 0.5, \tag{12}$$

where $\mathbf{I}_2$ and $\mathbf{I}_4$ are the 2×2 and 4×4 identity matrices, respectively. The number of generated particles is $N = 500$. The horizon size for the nonlinear FIR f lter included in the CPFF is set as $M = 4$. The sampling time interval T is set to $0.1s$. We assum that the initial person position is unknown (i.e., global localization). Thus, the initial particles for the PF are generated following the uniform distribution.

Figure 2 shows the localization results obtained using the above parameters. Figure 2(a) represents the real trajectory and the trajectories estimated by the PF and the CPFF. Figure 2(b) shows the localization errors, which are computed as

$$E_{\text{loc}} = \sqrt{(x_k - \hat{x}_k)^2 + (y_k - \hat{y}_k)^2}, \tag{13}$$

where (x_k, y_k) are the true coordinates of the person at time index k and $(\hat{x}_k, \hat{y}_k)$ are the estimated coordinates.

The simulation condition (i.e., parameter setting) is moderate, which means the measurement noise is moderate and the number of particles is suff ciently large. Under this condition, the PF works well and produces successful localization results. The highest localization error is about $0.17m$ at the initial time ($k = 1$). Although the localization error increases at the corners ($k = 100$, 200, and 300), overall localization errors are suff ciently small. PF failure (i.e., abnormally large localization errors) does not occur. Since no PF failure is detected, the CPFF operates as a pure PF. In Fig. 2(a) and 2(b), we can see that the PF and the CPFF produce similar localization results. We call this case "ideal."

Next, we assume that measurements are provided using an accurate WSN with very low noise. Ironically, an increase in the measurement accuracy enhances the sample impoverishment, resulting in PF

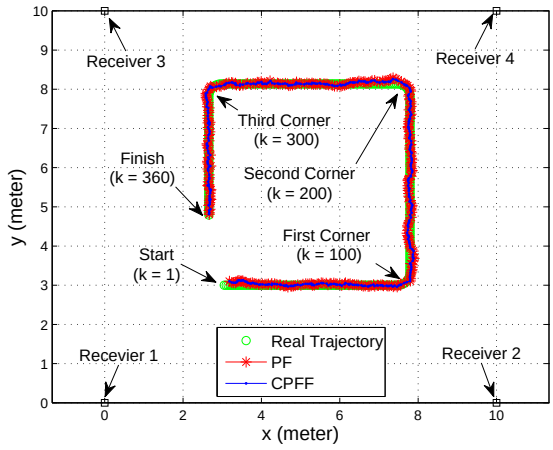

(a)

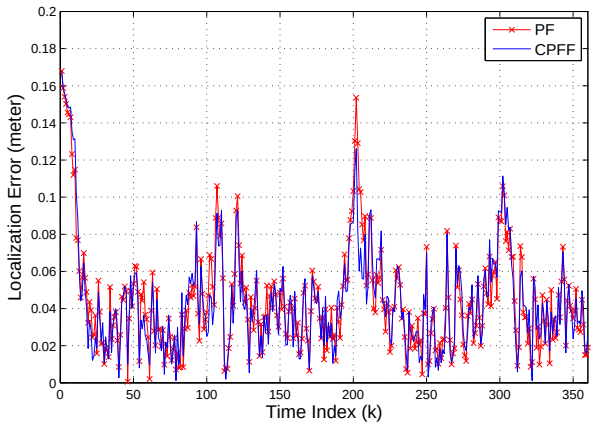

(b)

Figure 2: Indoor localization using PF and CPFF under "ideal" conditions: (a) real and estimated trajectories of person, and (b) localization errors.

performance degradation [6]. In that case, the PF becomes likely to produce unacceptable errors and even divergence [7, 11]. In the following subsections, we show that the CPFF eff ciently overcomes this problem.

We generate the measurement noise with $\sigma_v = 0.1$. As can be seen in Fig. 3(a), the PF loses its ability to track accurately at each point when a person changes trajectory abruptly. Figure 3(b) shows the localization errors. Because there is a large range of localization errors, we used the logarithmic scale. As seen in Fig. 3(b), low measurement noise causes extensive excursions in the localization errors produced by the PF. Note that the random-walk model used in this paper assumes a constant velocity as well as suggests that the modeling errors will grow if the person changes trajectory abruptly. By contrast, the proposed CPFF produces much smaller errors at the points of

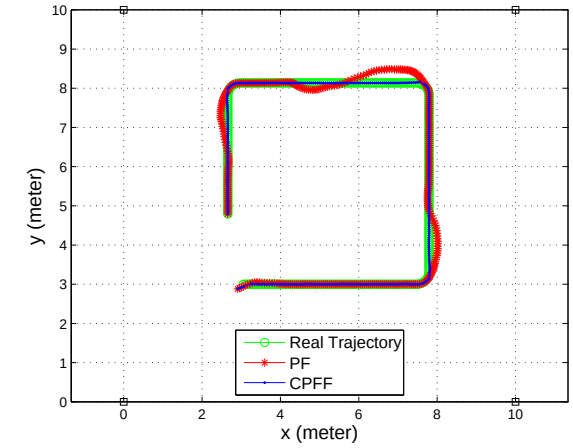

(a)

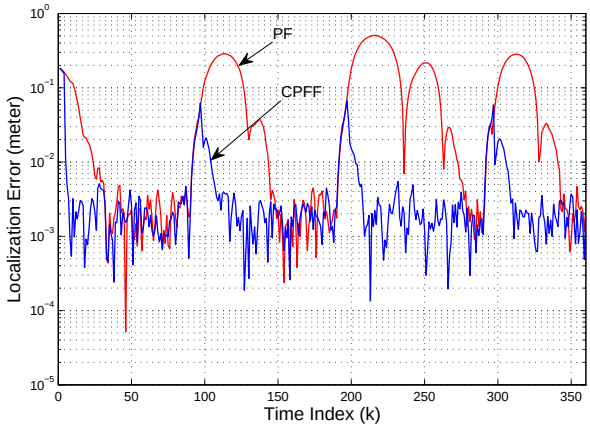

(b)

Figure 3: Indoor localization using PF and CPFF under low measurement noise condition ($\sigma_v = 0.1$): (a) real and estimated trajectories of person, and (b) localization errors.

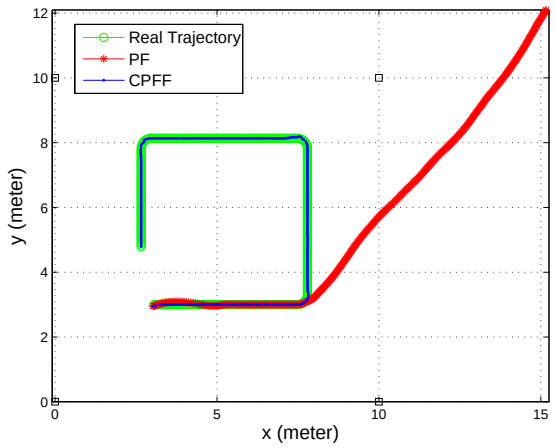

(a)

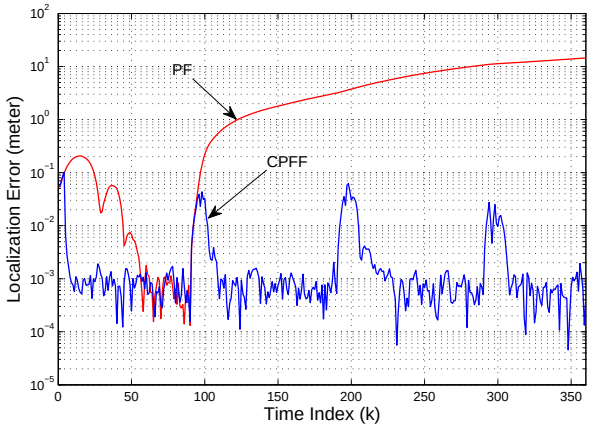

(b)

Figure 4: Indoor localization using PF and CPFF under very low measurement noise condition ($\sigma_v = 0.05$): (a) real and estimated trajectories of person, and (b) localization errors.

change, and we conclude that this f lter has much better robustness against abrupt changes in the person trajectory.

In the next simulation, we enforce the effect by reducing the measurement noise covariance to $\sigma_v = 0.05$. As shown in Fig. 4(a), with this harsh condition, the PF diverges at the f rst point of abrupt change and never returns to an actual trajectory. On the contrary, we do not observe this divergence in the proposed CPFF, even though it exhibits excursions in Fig. 4(b) at each point of abrupt change. Thus, the CPFF is also more stable than the pure PF. As seen in Figs. 3 and 4, the proposed CPFF successfully detects the localization failures and recovers the localization algorithm from failures.

5 Conclusion

In this paper, we proposed a new nonlinear f ltering algorithm called the CPFF. In indoor localization based on WSNs, the pure PF exhibited failures due to sample impoverishment, which is caused by low measurement noises. However, the proposed CPFF exhibited accurate localization results without failures compared with the pure PF. Since the CPFF can provide accurate and reliable localization results, it can effectively used in many indoor localization systems.

References:

[1] H. Liu, H. Darabi, P. Banerjee, and J. Liu, "Survey of wireless indoor positioning techniques and systems," *IEEE Trans. Systems, Man, and Cyber. C*, vol. 37, no. 6, pp. 1067–1080, Nov. 2007.

[2] W. Yu, J. Y. Lee, Y. G. Ha, M. Jang, J. C. Sohn, Y. M. Kwon, and H. S. Ahn, "Design and implementation of a ubiquitous robotic space," *IEEE Trans. Autom. Sci. Eng.*, vol. 6, no. 4, pp. 633–640, Oct. 2009.

[3] R. V. Kulkarni and G. K. Venayagamoorthy, "Bio-inspired algorithms for autonomous deployment and localization of sensor nodes," *IEEE Trans. Systems, Man, and Cyber. C*, vol. 40, no. 6, pp. 663–675, Nov. 2010.

[4] J. Pomarico-Franquiz and Y. S. Shmaliy, "Accurate self-localization in RFID tag information grids using FIR filtering," *IEEE Trans. Ind. Informat.*, vol. 10, no. 2, pp. 1317–1326, May 2014.

[5] J. Pomarico-Franquiz, S. H. Khan, and Y. S. Shmaliy, "Combined extended FIR/Kalman filtering for indoor robot localization via triangulation," *Measurement*, vol. 50, pp. 236–243, Apr. 2014.

[6] S. Thrun, W. Burgard, and D. Fox, *Probabilistic Robotics*, Cambridge, MA: The MIT Press, 2005.

[7] D. Simon, *Optimal State Estimation: Kalman, H_∞, and Nonlinear Approaches*, Hoboken, NJ: John Wiley & Sons, 2006.

[8] N. Oudjane and C. Musso, "Progressive correction for regularized particle filters," *Proc. 3rd Int. Conf. Information Fusion (Paris, France)*, 2000.

[9] W. R. Gilks and C. Berzuini, "Following a moving target - Monte Carlo inference for dynamic Bayesian models," *Journal of Royal Statistical Society: Series B (Statistical Methodology)*, vol. 63, no. 1, pp. 127–146, 2001.

[10] R. van der Merwe, A. Doucet, N. de Freitas, and E. Wan, "The unscented particle filter," *Tech. Rep. CUED/F-INFENG/TR 380*, Cambridge University Engineering Department, 2000.

[11] B. Ristic, S. Arulampalam, and N. Gordon, *Beyond the Kalman Filter: Particle Filters for Tracking Applications*, Norwood, MA: Arctech House, 2004.

[12] Y. S. Shmaliy, "Unbiased FIR filtering of discrete-time polynomial state-space models," *IEEE Trans. Signal Process.*, vol. 57, no. 4, pp. 1241–1249, Apr. 2009.

[13] Y. S. Shmaliy, "Linear optimal FIR estimation of discrete time-invariant state-space models," *IEEE Trans. Signal Process.*, vol. 58, no. 6, pp. 3086–3096, Jun. 2010.

[14] Y. S. Shmaliy, "An iterative Kalman-like algorithm ignoring noise and initial conditions," *IEEE Trans. Signal Process.*, vol. 59, no. 6, pp. 2465–2473, Jun. 2011.

[15] Y. S. Shmaliy, "Suboptimal FIR filtering of nonlinear models in additive white Gaussian noise," *IEEE Trans. Signal Process.*, vol. 60, no. 10, pp. 5519–5527, Oct. 2012.

[16] D. Simon and Y. S. Shmaliy, "Unified forms for Kalman and finite impulse response filtering and smoothing," *Automatica*, vol. 49, no. 6, pp. 1892–1899, Jun. 2013.

[17] F. Ramirez-Echeverria, A. Sarr, and Y. S. Shmaliy, "Optimal memory of discrete-time FIR filters in state-space," *IEEE Trans. Signal Process.*, vol. 62, no. 3, pp. 557–561, Feb. 2014.

[18] S. Zhao and Y. S. Shmaliy, "Fast computation of discrete optimal FIR estimates in white Gaussian noise," *IEEE Trans. Signal Process. Lett.*, vol. 22, no. 6, pp. 718–722, Jun. 2015.

[19] C. K. Ahn, S. Han, and W. H. Kwon, "H_∞ FIR filters for linear continuous-time state-space systems," *IEEE Signal Process. Lett.*, vol. 13, no. 9, pp. 557–560, Sep. 2006.

[20] C. K. Ahn, S. Han, and W. H. Kwon, "H_∞ finite memory controls for linear discrete-time state-space models," *IEEE Trans. on Circuits & Systems II*, vol. 54, no. 2, pp. 97–101, 2007.

[21] C. K. Ahn, "Strictly passive FIR filtering for state-space models with external disturbance," *Inter. Journ. of Electron. and Commun.*, vol. 66, no. 11, pp. 944–948, Nov. 2012.

[22] C. K. Ahn, "A new solution to the induced l_∞ finite impulse response filtering problem based on two matrix inequalities," *Intern. Journ. of Contr.*, vol. 87, no. 2, pp. 404–409, 2014.

[23] J. M. Pak, C. K. Ahn, M. T. Lim, and M. K. Song, "Horizon group shift FIR filter: alternative nonlinear filter using finite recent measurements," *Measurement*, vol. 57, pp. 33–45, November 2014.

[24] J. M. Pak, S. Y. Yoo, M. T. Lim, and M. K. Song, "Weighted average extended FIR filter bank to manage the horizon size in nonlinear FIR filtering," *International Journal of Control, Automation, and Systems*, vol. 13, no. 1, pp. 138–145, Feb. 2015.

[25] J. M. Pak, C. K. Ahn, Y. S. Shmaliy, P. Shi, and M. T. Lim, "Switching extensible FIR filter bank for adaptive horizon state estimation with application," *IEEE Trans. on Control Systems Technology* (In press, DOI: 10.1109/TCST.2015.2472990), 2015.

[26] J. M. Pak, C. K. Ahn, C. J. Lee, P. Shi, M. T. Lim, and M. K. Song, "Fuzzy horizon group shift FIR filtering for nonlinear systems with Takagi-Sugeno model," *Neurocomputing*, vol. 174, Part B, pp. 1013–1020, Jan. 2016.

[27] J. M. Pak, C. K. Ahn, P. Shi, and M. T. Lim, "Self-recovering extended Kalman f ltering algorithm based on model-based diagnosis and resetting using an FIR f lter," *Neurocomputing*, vol. 173, Part 3, pp. 645–658, Jan. 2016.

[28] I. H. Choi, J. M. Pak, C. K. Ahn, Y. H. Mo, M. T. Lim, and M. K. Song, "New preceding vehicle tracking algorithm based on optimal unbiased f nite memory f lter," *Measurement*, vol. 73, pp. 262–274, Sep. 2015.

[29] I. H. Choi, J. M. Pak, C. K. Ahn, S. H. Lee, M. T. Lim, and M. K. Song, "Arbitration algorithm of FIR f lter and optical f ow based on ANFIS for visual object tracking," *Measurement*, vol. 75, pp. 338–353, Nov. 2015.

[30] C. J. Lee, J. M. Pak, C. K. Ahn, K. M. Min, P. Shi, and M. T. Lim, "Multi-target FIR f ltering algorithm for Markov jump linear systems based on true-target decision-making" *Neurocomputing*, vol. 168, pp. 298–307, Nov. 2015.

[31] J. M. Pak, C. K. Ahn, Y. S. Shmaliy, P. Shi, and M. T. Lim, "Accurate and Reliable Human Localization Using Composite Particle/FIR Filtering," Submitted to *IEEE Trans. Human-Machine Systems*, 2016.

[32] A. S. Paul and E. A. Wan, "RSSI-based indoor localization and tracking using sigma-point Kalman smoothers," *IEEE J. Sel. Topics Signal Process.*, vol. 3, no. 5, pp. 860–873, Oct. 2009.

[33] P. C. Mahalanobis, "On the generalised distance in statistics," *Proceedings of the National Institute of Sciences, Calcutta, India*, Apr. 1936.

[34] S. K. Singh, M. Premalatha, and G. Nair, "Ellipsoidal gating for an airborne track while scan radar," *Proc. of IEEE 1995 Int. Radar Conf.*, pp. 334–339, May. 1995.

[35] R. C. Smith and P. Cheeseman, "On the representation and estimation of spatial uncertainty," *The International Journal of Robotics Research*, vol. 5, no. 4, pp. 56–68, Winter 1986.